J Mater Sci: Mater Med (2009) 20:S223–S227
DOI 10.1007/s10856-008-3533-z

Load sensing surgical instruments

C. Jacq · T. Maeder · P. Ryser

Received: 13 September 2007 / Accepted: 8 July 2008 / Published online: 5 August 2008

Abstract Force and pressure sensing technology applied to smart surgical instruments as well as implants allow to give a direct feedback of loads to the surgeon lead to better reliability and success of surgical operations. A common technology used for sensors is low-cost piezoresistive thick-film technology. However, the standard thick-film firing conditions degrade the properties of medical alloys. In order to avoid this problem, the solution is to decrease the firing temperature of thick films. This work presents the development and characterisation of low-firing thick-film systems (dielectrics, resistors and conductors), formulated to achieve chemical and thermal expansion compatibility with an austenitic stainless steel medical alloy. Adherence tests and results on electrical properties of these systems: resistance, temperature coefficient of resistance (TCR) are presented. It was found that the main issue in these systems lies in mastering the materials interactions during firing, especially at the silver-based resistor terminations. The interaction of silver, resistor and dielectric tends to give rise to highly resistive zones at the terminations, affecting reliability. This can be circumvented by post-firing the resistor terminations at a moderate temperature.

1 Introduction

The overall object of this project is the application of force and pressure sensing technology to smart surgical instruments as well as implants. Smart instruments allowing direct feedback of loads to the surgeon lead to better reliability and success of surgical operations. Load-sensing implants are to be a useful tool in monitoring patient recovery in cases such as bone fracture, and also in aiding the re-education process.

A well established and low production cost solution for force and pressure sensing is thick-film piezoresistive technology, usually applied on ceramic substrates. However, alumina is not optimal for piezoresistive sensing applications, as it is brittle, its elastic modulus high and its strength rather low, compared to metallic materials such as high-strength stainless steels and Ti alloys [1, 2], which are commonly applied for medical devices such as instruments, fixtures and implants.

Thick-film piezoresistive sensors on metallic substrates have been investigated previously [3], and used to fabricate a ligament balancing sensor for total knee arthroplasty (TKA) [4–6]. However, the standard thick-film firing temperature (850°C) is not compatible with Ti alloys, which oxidise too extensively. Stainless steels, on the other hand, undergo degradation of mechanical properties due to annealing or phase transformations incompatible with the presence of thick-film layers.

Medical-grade austenitic stainless steels with nitrogen additions, such as the alloy used for the TKA sensor [4–6], do not undergo phase transformations, and nitrogen allows reasonable strength even in the annealed state. However, mechanical properties remain suboptimal, and these alloys have a very high coefficient of thermal expansion (CTE), ca. 17 ppm/K (vs. 11 for ferritic/martensitic steels and 7 for alumina). Therefore, standard thick-film materials tend to have poor reliability due to excessive stresses. That's why, a specific materials system, with a low firing temperature to conserve mechanical properties and with a CTE matched to that of the steel, is highly desirable.

C. Jacq (✉) · T. Maeder · P. Ryser
Laboratoire de Production Microtechnique, Ecole Polytechnique Fédérale de Lausanne, BM – Station 17, 1015 Lausanne, Switzerland
e-mail: caroline.jacq@epfl.ch

In previous studies [7–10], we have developed and studied several such low-firing systems based on low-melting lead borosilicate glasses, where the materials were formulated to achieve compatibility with a wide range of substrates such as glass, aluminium metal and steels. CTE matching (which is important mainly for the insulating dielectric) was successfully achieved by adjusting the glass composition, the filler and the loading. One remaining problem was the presence of highly resistive zones near the resistor terminations, which is deleterious to reproducibility and reliability. This was mitigated on a system optimised for ferritic/martensitic stainless steels by post-firing the terminations at a low temperature and/or through Bi_2O_3 additions to the materials [11].

In this work, we therefore endeavour to systematically investigate the termination effect for our low-firing thick-film system adapted to austenitic steels (e.g. with a different formulation of the insulating dielectric), in the light of the previous study [11]. Additional integration issues such as adherence and conductor pad solderability are also studied.

2 Experimental

The following substrate materials were used: 96% pure alumina (Kyocera, Japan, A-476) as standard thick-film substrate and austenitic stainless steel 1.4435 (comparable to the medical alloy used for the sensor). The steel substrates were pre-oxidised at 900°C during 1 h in order to increase the adherence of the dielectrics.

All dielectric materials used in this work are based on the lead borosilicate glass ("V6") used in our previous studies [7–12]: 75% PbO + 10% B_2O_3 + 15% SiO_2 (mass%) with 2% Al_2O_3 added to inhibit crystallisation [13].

The basic dielectric sequence (variant "C") starts with a first layer with 25% vol. Fe_2O_3 as an adhesion promoter, followed by 2 layers filled with cristobalite (Quarzwerke, Sikron cristobalite flour SF8000 D50:2.5 μm particle size).

Two modifications to the top layer of this dielectric sequence, which is in contact with the resistor, were examined: (1) replacing the cristobalite filler with alumina (C → A, Alfa Aesar, aluminium oxide alpha, 99.99%, 1 μm), and/or (2) doping with Bi_2O_3 added as powder to the paste (C, A → C_{Bi}, A_{Bi}, Alpha Aesar 12230, 99%). The volume fractions and codes of the resulting dielectrics are given in Table 1. Together with the option of firing on bare alumina, this gives 5 dielectric + substrate variants. All the dielectric layers were fired separately at a peak temperature of 625°C, with a 10 min dwell.

As pre-fired Ag conductors were found to give rise to undesirable high-resistivity zones near the terminations with our materials [11], we take in the present work the option of post-firing the terminations at a temperature lower than the one used for the resistor firing. A commercial Ag conductor material allowing a reduced firing temperature was applied: ESL 9912A, fired at 600°C/10 min. Additionally, the possibility of using a very low-firing (500°C) conductor, consisting of Ag powder (Nanostrutured & Amorphous Materials Inc. 99.9%, APS 30 nm) with a very low-melting glass binder ("V8", 85% PbO + 10% - B_2O_3 + 5% SiO_2, mass%, + 2% Al_2O_3 [7–11]) was examined. As in the case of the dielectrics, doping with Bi_2O_3 was also examined. The resulting 4 conductors + firing order variants are given in Tables 1 and 2.

For the resistive composition, a commercial low-firing 10 kΩ paste, ESL 3114, was used, also with or without Bi_2O_3 doping (Table 1). In this study, the resistors were always fired at 625°C/10 min.

Two firing sequences, differing by the number of resistor firings, were also compared (Table 2).

Samples for sheet resistance and temperature coefficient of resistance (TCR) were 1.5 mm wide resistors of several lengths (Fig. 1), and were measured at 30°C, 65°C and 100°C.

As in the previous study [11], termination effects were compared through a "length index" LI, defined as the ratio of the average sheet resistance of the three short resistors (0.3, 0.6 and 1.0 mm length) to the average of the 1.5 mm long ones. LI values greater than 1 imply the existence of highly resistive zones near the terminations, whereas the

Table 1 List of materials

Designation	Description (numbers in volume %)
Substrate + dielectrics	
*	(alumina substrate)
C	40 V6 + 60 Cristobalite
C_{Bi}	32 V6 + 58 Cristobalite + 10 Bi_2O_3
A	50 V6 + 50 Al_2O_3
A_{Bi}	40 V6 + 50 Al_2O_3 + 10 Bi_2O_3
Conductors and order	
V	100 ESL 9912A
V_{Bi}	85 ESL 9912A + 15 Bi_2O_3
W	90 Ag + 10 V8
W_{Bi}	83 Ag + 7 V8 + 10 Bi_2O_3
Resistors	
R	100 ESL 3114
R_{Bi}	90 ESL 3114 + 10 Bi_2O_3

Table 2 Firing sequences

Dielectric 625°C	Resistor 625°C	Conductor 500°C	Conductor reinforcement 500°C
Dielectric 625°C	Resistor and Conductor reinforcement 625°C	Conductor 500°C	

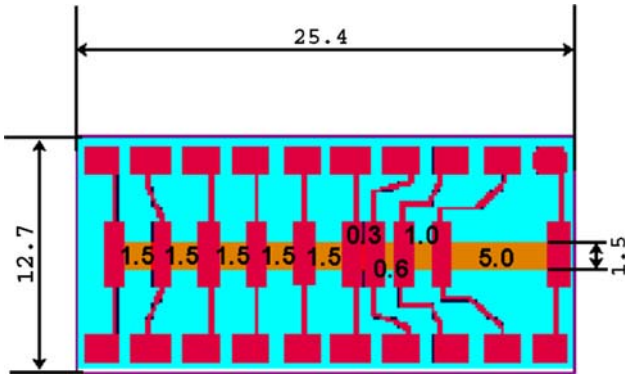

Fig. 1 Layout of the test sample for measurement of electrical properties

other case (LI < 1) corresponds to a locally decreased sheet resistance near the terminations.

3 Results and discussions

The results for length index LI, sheet resistance R_s and TCR are compiled in Tables 3, 4 and 5 respectively.

The most important factor is the firing temperature of the terminations. ESL 9912A (variants V & V_{Bi}), doped or not with Bi_2O_3 fired at 600°C, is not suitable for the terminations, as LI is very high for all variants with this conductor. On the other hand, the low-firing (500°C) terminations (W & W_{Bi}) minimise interdiffusion and exhibit LI values close to 1, indicating much smaller termination effects. Also, TCR values also exhibit little influence of length. We will therefore concentrate the rest of the discussion on these samples.

The number of firings of the resistors (2 or 3, with 1 or 2 refires at 500°C) has some influence: while TCR and LI are little affected, a second refire increases resistance around 15%.

Doping the resistors and the dielectric with Bi_2O_3 strongly decreases both sheet resistance and TCR on steel, and only sheet resistance on alumina. Bi_2O_3 in the dielectric has a smaller effect, and probably acts through diffusion of this oxide into the resistor (this is supported by the fact that the effect on Bi_2O_3-doped resistors is much smaller). This decrease of resistivity occurs in spite of the corresponding dilution effect. Therefore, Bi_2O_3 clearly interacts with the resistor material and lowers its resistivity, probably by dissolving into the lead borosilicate glass matrix, which has an effect analogous to an increase of PbO in the glass [14, 15]. On the other hand, adding Bi_2O_3 to the conductor has nearly no influence on the electrical properties (W vs. W_{Bi}), except a slight decrease of TCR when Bi is absent from both dielectric and resistor.

The type of filler in the dielectric also has a significant effect: resistance is lower and TCR more positive with alumina than with cristobalite filler. This is ascribed to differences of chemical reactivity: alumina is very inert, whereas cristobalite, a form of SiO_2, will tend to dissolve partially into the resistor glass.

Overall, if one considers Bi_2O_3 to be analogous to PbO, our observations are in line with that of Adachi and Kuno [16], who found that resistivity is high with low-lead (high SiO_2) glasses, and low with high-lead ones.

Figure 2 illustrates the dependence of sheet resistance with the length of resistance. Size effects have been completely circumvented by using the low temperature fired conductor.

Pull tests have been used to evaluate the adherence and the solderability of the thick-film conductors. Both conductors V and W have been tested with SN96 solder (96.5% Sn–3.5% Ag). The force at rupture has been measured on the four dielectrics and alumina substrate as reference. The results are depicted on the Fig. 3.

The V conductor (ESL 9912A) could not be tested on alumina substrate because this conductor requires 850°C to

Table 3 Length index LI

Cond. and order Sub. + diel. + res.	Resistor fired 3 times				Resistor fired 2 times	
	V	V_{Bi}	W	W_{Bi}	W	W_{Bi}
* + R	1.41	1.47	0.87	0.90	0.95	0.91
* + R_{Bi}	1.49	1.59	1.07	1.09	1.1	1.01
C + R	1.91	2.05	0.99	0.94	0.9	0.94
C + R_{Bi}	2.61	2.54	1.06	1.08	1.01	0.99
C_{Bi} + R	2.27	2.12	0.94	0.91	0.97	0.94
C_{Bi} + R_{Bi}	2.22	2.42	1.02	1.12	1.10	1.02
A + R	3.44	2.62	1.00	1.03	1.01	0.99
A + R_{Bi}	2.99	3.17	1.09	1.10	1.09	1.05
A_{Bi} + R	2.31	3.12	1.07	1.07	0.98	0.96
A_{Bi} + R_{Bi}	3.09	2.77	1.23	1.16	1.12	1.14

Table 4 Sheet resistance Rs (kΩ)

Cond. and order Sub. + diel. + res.	Resistor fired 3 times				Resistor fired 2 times	
	V	V_{Bi}	W	W_{Bi}	W	W_{Bi}
* + R	16.68	22.3	12.4	12.39	10.62	9.97
* + R_{Bi}	5.68	5.29	3.82	3.80	3.31	3.46
C + R	32.35	33.25	13.79	13.85	11.68	11.6
C + R_{Bi}	22.36	20.55	8.31	7.54	7.3	6.58
C_{Bi} + R	21.53	18.74	8.1	8.24	6.88	6.96
C_{Bi} + R_{Bi}	28.48	23.28	6.43	6.8	6.5	5.66
A + R	41.78	33.55	7.51	7.96	6.52	6.84
A + R_{Bi}	21.37	15.78	4.01	3.97	3.85	3.90
A_{Bi} + R	19.19	16.34	4.39	4.36	3.93	4.1
A_{Bi} + R_{Bi}	14.79	12.17	3.51	3.41	3.07	2.99

Table 5 Temperature coefficient TCR (ppm/K)

Cond. and order Sub. + diel. + res.	Resistor fired 3 times				Resistor fired 2 times	
	V	V_{Bi}	W	W_{Bi}	W	W_{Bi}
* + R	−285	−286	−263	−292	−274	−263
* + R_{Bi}	−273	−269	−267	−264	−274	−274
C + R	49	71	−46	−72	−52	−57
C + R_{Bi}	−119	−113	−135	−139	−127	−125
C_{Bi} + R	−15	−5	−74	−83	−65	−70
C_{Bi} + R_{Bi}	−120	−134	−136	−123	−126	−130
A + R	97	102	36	23	48	38
A + R_{Bi}	−10	−2	−31	−35	−31	−24
A_{Bi} + R	17	31	5	0	10	9
A_{Bi} + R_{Bi}	−15	−8	−4	−7	2	5

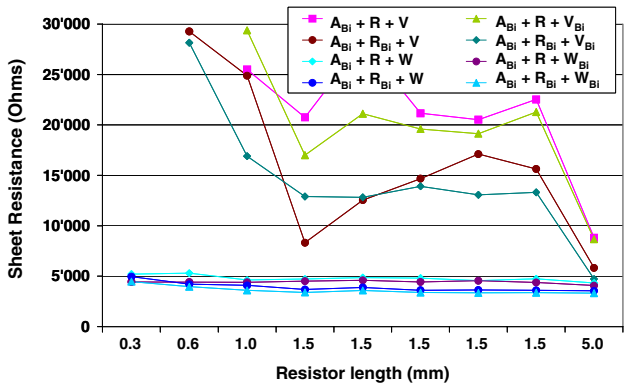

Fig. 2 Evolution of sheet resistance with length of resistors

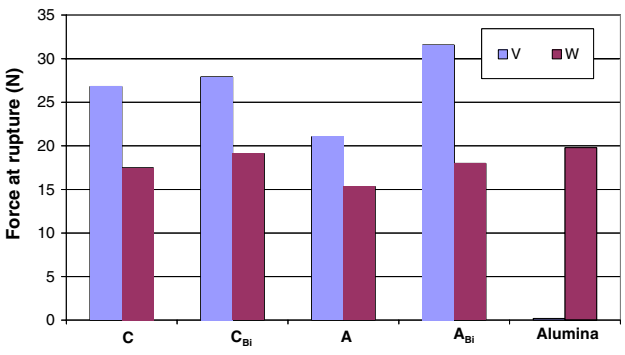

Fig. 3 Adherence test on 1.4435 steel

adhere to this substrate. On the other hand, this conductor gives the best adhesion strength on dielectric, which is due to better wettability of the solder, which is facilitated by the low glass content of this conductor. During the pull test, fracture occurs both in the dielectric and the conductor. Therefore, the most favourable solution for applications is to co-fire ESL 9912A solder pads with the resistor, and then apply (post-fire) low-firing Ag for the resistor terminations.

The Fe_2O_3 was found to be an efficient adhesion promoter for dielectric on steel; failure nearly never occurs at the metal–dielectric interface, but mostly in the dielectric or at the conductor/dielectric interface. The beneficial effects of Fe_2O_3 are thought to be due to it preventing the occurrence of reducing conditions at the metal–dielectric

interface through a redox mechanism. Similar results may be obtained with oxides of Ni, Cu, Mn, Co, etc.

4 Conclusions and outlook

The goal of this work was to study low-firing thick-film materials for piezoresistive sensor applications on medical-grade austenitic stainless steels, and achieve a reliable system.

Previously occurring issues with highly resistive zones near the silver terminations have been solved by developing conductors post-fireable at a low temperature (500°C), although stability of this solution must be studied in the future.

Dielectrics filled with cristobalite were used to match the CTE of the substrate, but were found to somewhat interact with the resistors. In order to reduce this effect, a top layer filled with alumina was added as a diffusion barrier.

Doping the dielectric and/or the resistive material (ESL 3114) with Bi_2O_3 was found to strongly reduce the resistivity. The effect on the piezoresistive properties must still be elucidated.

For a good solderability and adherence, the conductor ESL 9912A fired with the resistors is the best conductor for a solder connection, and the Fe_2O_3 filler guaranteed good adhesion of the dielectric to the steel.

Although the sensors are coated with parylene to render them biocompatible [6], the presence of lead-based materials within medical sensors, even in a relatively insoluble glass matrix, is a cause of concern. Therefore, future work will focus on the elimination of lead from the glass matrix used in this thick-film system.

References

1. C. Jacq, T. Maeder, P. Ryser, J. Europ. Ceramic Soc. **4**(6), 1897–1900 (2004)
2. T. Maeder, H. Birol, C. Jacq, P. Ryser, in *Proceedings, European Microelectronics and Packaging Symposium,* Prague (CZ), 2004, pp. 272–276
3. N.M. White, Thesis, University of Southampton, Faculty of Engineering & Applied Science (1988)
4. D. Crottet, T. Maeder, D. Fritschy, H. Bleuler, L.P. Nolte, I.P. Pappas, IEEE Trans. Biomed. Eng. **52**(9), 1609–1611 (2005)
5. D. Crottet, J. Kowal, S.A. Sarfert, T. Maeder, H. Bleuler, L.P. Nolte, L. Dürselen, J. Biomech. **40**(8), 1709–1715 (2007)
6. D. Crottet, T. Maeder, S.A. Sarfert, D. Fritschy, H. Bleuler, L.P. Nolte, I.P. Pappas, *51st Annual Meeting of the Meeting of the Orthopaedic Research Society*, Washington (USA), (2005)
7. C. Jacq, T. Maeder, S. Martinerie, G. Corradini, E. Carreño-Morelli, P. Ryser, in *Proceedings, 4th European Microelectronics and Packaging Symposium*, Terme Čatež (SI), IMAPS, 2006, pp. 105–109
8. C. Jacq, S. Vionnet, T. Maeder, P. Ryser, in *Proceedings, European Microelectronics and Packaging Symposium*, Prague (CZ), 2004, pp. 267–271
9. C. Jacq, T. Maeder, S. Vionnet, P. Ryser, J. Europ. Ceramic Soc. **25**(12), 2121–2124 (2005)
10. C. Jacq, T. Maeder, S. Menot-Vionnet, H. Birol, I. Saglini, P. Ryser, in *Proceedings of the 15th European Microelectronics and Packaging Conference (EMPC)*, Brugge (BE), IMAPS, 2005, pp. S13.04, 319–324
11. C. Jacq, T. Maeder, N. Johner, G. Corradini, P. Ryser, in *Proceedings of the 16th European Microelectronics and Packaging Conference (EMPC)*, Oulu, (FI), IMAPS, pp. 167–170
12. S. Vionnet-Menot, C. Grimaldi, T. Maeder, P. Ryser, S. Strässler, Phys. Rev. B **71**, 064201 (2005)
13. M. Prudentiati, B. Morten, B. Forti, A.F. Gualtieri, G.M. Dilliway, Inter. J. Inorg. Mater. **3**, 667–674 (2001)
14. M. Hamezan, H.A.A. Sidek, A.W. Zaidan, K. Kaida, A.T. Zainal, J. Appl. Sci. **6**(4), 943–949 (2006)
15. G.E. Rachkovskaya, G.B. Zakharevich, Glass Ceram. **61**(1–2), 9–12 (2004)
16. K. Adachi, H. Kuno, J. Am. Ceramic Soc. **83**(10), 2441–2448 (2000)